Closed-form Solution to Directly Design FACE Waveforms for Beampatterns Using Planar Array

Taha Bouchoucha, Sajid Ahmed, *Senior Member, IEEE*,
Tareq Al-Naffouri, *Member, IEEE*, and Mohamed-Slim Alouini, *Fellow, IEEE*
Computer, Electrical, Mathematical Sciences and Engineering (CEMSE) Division
King Abdullah University of Science and Technology (KAUST)
Thuwal, Makkah Province, Saudi Arabia
Emails: sajid.ahmed, slim.alouini@kaust.edu.sa
Phone: +966 (012) 808-0286, +966 (012) 808-0283
EDICS: SAM-APPL, SAM-RADR

***Abstract*—In multiple-input multiple-output radar systems, it is usually desirable to steer transmitted power in the region-of-interest. To do this, conventional methods optimize the waveform covariance matrix, R, for the desired beampattern, which is then used to generate actual transmitted waveforms. Both steps require constrained optimization, therefore, use iterative algorithms. The main challenges encountered in the existing approaches are the computational complexity and the design of waveforms to use in practice. In this paper, we provide a closed-form solution to design covariance matrix for the given beampattern using the planar array, which is then used to derive a novel closed-form algorithm to directly design the finite-alphabet constant-envelope (FACE) waveforms. The proposed algorithm exploits the two-dimensional fast-Fourier-transform. The performance of our proposed algorithm is compared with existing methods that are based on semi-definite quadratic programming with the advantage of a considerably reduced complexity.**

***Index Terms*—Multiple-input multiple-output radars, beampattern design, closed-form solution, waveform design, two-dimensional fast-Fourier-transform.**

I. Introduction

Colocated multiple-input multiple-output (MIMO) radar has a number of advantages over the classical phased-array radars. For example, it yields significant improvement in parameter identifiability, allows detecting a higher number of targets and provides enhanced flexibility to design transmit beampatterns [1]–[6]. In fact, the design of transmit beampatterns has lately attracted extensive attention. In the transmit beampattern design problem, we aim to focus the transmitted power in a certain region-of-interest (ROI) [7]–[12]. This process turns out to be essential in a number of applications. For example, imaging radars, generally focus the transmitted power in the pre-defined ROI on the ground but may receive reflected signals out of the ROI due to the side-lobes of its antenna [13]. Therefore, it is necessary to focus as much as possible the transmitted power only in the ROI.

It is known that the transmit beampattern of a colocated antenna array depends on the cross-correlation between the transmitted waveforms from different antennas. Therefore, to design variety of transmit beampatterns, early solutions have relied on a two-step process [7]–[12]. In the first step, user designs the waveforms covariance matrix such that the theoretical transmitted power matches the desired beampattern as closely as possible. The second step then involves the design of the actual waveforms that can realise the designed covariance matrix. Both of these steps require constrained optimisation and most of the available literature uses iterative algorithms. To match the desired beampatterns, the waveforms can also be designed directly without synthesizing the covariance matrix. However, as far as the authors know, optimal solutions to directly design the waveforms for a given beampattern are not available yet.

Using the first approach, to synthesise the waveform covariance matrix for the given beampattern, efficient algorithms are proposed in [8], [11], [14]. All of them are iterative approaches optimising some constrained problems. These algorithms are computationally very expensive for real-time applications. A closed form solution, to find the waveform covariance matrix, which is based on fast-Fourier-transform (FFT) has been lately proposed in [15]. Once the covariance matrix is synthesized, the corresponding waveforms fulfilling some practical constraints such as close to unity peak-to-average power ratio (PAPR) are designed. To design such waveforms an algorithm is proposed in [16]. This algorithm is also iterative in nature with a very high computational complexity. In addition, it generates non-finite alphabets that can be challenging to use in practice. In [17], the authors proposed a closed-form and an iterative solution to generate best possible finite-alphabet constant-envelope (FACE) waveforms to realize the given covariance matrix. In this algorithm, mapping of Gaussian random variables onto binary phase-shift keying (BPSK) symbols is exploited. The main drawback of this algorithm is that its performance is beampattern dependent.

Using the second approach, which consists in directly designing the waveforms for a uni-modal symmetric beampattern, a sub-optimal algorithm is presented in [18]. In this algorithm, a scalar coefficient is chosen to control the width of the beampattern. This method requires a high number of transmitting antennas in order to achieve a good performance to match the desired beampattern.

We have noticed that the solutions proposed in the previous work deal only with linear array and the ROI is defined by only one parameter which is the azimuth angle θ. In the planar array radar systems, the transmitting antennas form a plan and an additional dimension called the elevation angle ϕ is taken into account in order to provide a larger radar aperture. This allows to characterize the ROI in the three-dimensional (3D) space. In [12], various strategies for Hybrid MIMO phased-array radar, based on multiplication of signal sets by a pseudo-noise spreading sequence, are proposed for different transmit 3D beampatterns.

In this paper, we present a closed-form solution to design the waveform covariance matrix, for the desired 3D beampatterns, using a planar array radar. It is very expensive to synthesize waveform covariance matrix for large size planar array using semi-definite quadratic programming (SQP). Therefore, to reduce the computational complexity, the 3D beampattern design problem is mapped onto the two dimensional (2D) fast-Fourier-transform (2D-FFT). The algorithm in [15] can be considered as a special case of our proposed algorithm. Next, for the desired beampattern, by exploiting the derivations of covariance matrix in the proposed algorithm, a novel method to directly design the finite-alphabet constant-envelop (FACE) waveforms is also proposed. The direct design of waveforms does not require the synthesis of covariance matrix and the performance is same compared with the method using covariance matrix. Therefore, the proposed direct design of the waveforms yields significant reduction in computational complexity and can achieve the best possible performance among the existing direct waveform design algorithms.

The rest of this paper is organized as follows. In Sec. II, we present the signal model adopted for the planar array and formulate the optimization problem for the beampattern design. In Sec. III, by exploiting 2D-FFT, an algorithm to design covariance matrix for the desired beampattern is presented. Computational complexity to design covariance matrix using our proposed algorithm and SQP method is presented in Sec. IV. The direct design of the waveforms is discussed in Sec. V. Simulation results are discussed in Sec. VI, and conclusions are finally drawn in Sec. VII.

Notations: Small letters, bold small letters, and bold capital letters respectively designate scalars, vectors, and matrices. If $\mathbf{A}$ is a matrix, then $\mathbf{A}^H$ and $\mathbf{A}^T$ respectively denote the Hermitian transpose and the transpose of $\mathbf{A}$. $v(i)$ denotes the i^{th} element of vector $\mathbf{v}$. $A(i,j)$ denotes the entry in the i^{th} row and j^{th} column of matrix $\mathbf{A}$. The Kronecker product is denoted by $\otimes$. Modulo M operation on an integer i is denoted by $\langle i \rangle_M$ and $\lfloor i \rfloor_M$ denotes the quotient of i over M. Finally, the statistical expectation is denoted by $\mathrm{E}\{\cdot\}$.

II. System Model and Problem Formulation

Consider a MIMO radar system with a rectangular planar-array, composed of $M \times N$ omnidirectional antennas, placed at the origin of a unit radius sphere. As shown in Fig. 1, the inter-element-spacing (IES) between any two adjacent antennas in the x and y-axis directions is d_x and d_y, respectively. If a spatial location around this planar-array has an azimuth angle θ and an elevation angle ϕ, the corresponding Cartesian coordinates of a this location can be written as

$$\begin{aligned} x &= \sin(\phi)\cos(\theta), \\ y &= \sin(\phi)\sin(\theta), \end{aligned}$$

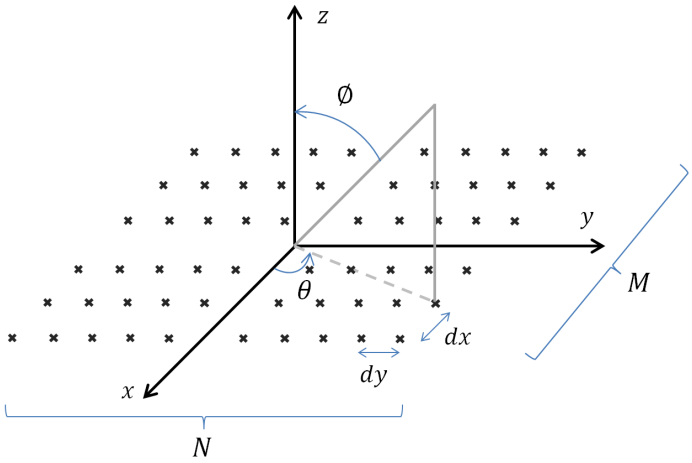

Fig. 1: Linear planar array of $M \times N$ transmit antennas.

Now we define the baseband transmitted signal vector containing the transmitted symbols from all antennas at time index n as

$$\mathbf{x}(n) = [x_{0,0}(n), \ldots, x_{0,N-1}(n), \ldots, x_{M-1,N-1}(n)]^T, \quad (1)$$

where $x_{p,q}(n)$ denotes the transmitted symbol from the antenna at the $(p,q)^{\text{th}}$ location at time index n. For narrow band signals with non-dispersive propagation, the signal received by a target located at location defined by the azimuth angle θ and the elevation angle ϕ can be written as

$$\begin{aligned} r(n;\theta,\phi) &= \sum_{p=0}^{M-1}\sum_{q=0}^{N-1} x_{p,q}(n)\, e^{j2\pi \frac{d_x(p,q)\sin(\phi)\cos(\theta)}{\lambda}} \\ &\quad e^{j2\pi \frac{d_y(p,q)\sin(\phi)\sin(\theta)}{\lambda}}. \end{aligned} \quad (2)$$

Assume that the distance between any two adjacent antennas on the x-axis and y-axis direction is $\lambda/2$, $d_x(p,q) = q\ \lambda/2$ and $d_y(p,q) = p\ \lambda/2$. This simplifies (2) to

$$r(n;\theta,\phi) = \sum_{p=0}^{M-1}\sum_{q=0}^{N-1} x_{p,q}(n)\, e^{j2\pi q\frac{\sin(\phi)\cos(\theta)}{2}} e^{j2\pi p\frac{\sin(\phi)\sin(\theta)}{2}}.$$

By exploiting the relationship between the spherical and Cartesian coordinates, given in (1), one can write the received signal in terms of Cartesian coordinates as

$$r(n;f_x,f_y) = \sum_{p=0}^{M-1}\sum_{q=0}^{N-1} x_{p,q}(n) e^{j2\pi(qf_x+pf_y)}, \quad (3)$$

where

$$\begin{aligned} f_x &= \frac{\sin(\phi)\cos(\theta)}{2}, \\ f_y &= \frac{\sin(\phi)\sin(\theta)}{2} \end{aligned} \quad (4)$$

are the normalised Cartesian coordinates of the same spatial location. It should be noted here that $-0.5 \leq \{f_x, f_y\} \leq +0.5$. The received signal in (3) can be written in vector form as

$$r(n; f_x, f_y) \quad = \quad \mathbf{a}_s^H(f_x, f_y)\, \mathbf{x}(n), \tag{5}$$

where

$$\mathbf{a}_s(f_x, f_y) = \begin{bmatrix} 1 \\ e^{j2\pi f_y} \\ \vdots \\ e^{j2\pi(M-1)f_y} \end{bmatrix} \otimes \begin{bmatrix} 1 \\ e^{j2\pi f_x} \\ \vdots \\ e^{j2\pi(N-1)f_x} \end{bmatrix}. \tag{6}$$

Using (3), the received power at the location (f_x, f_y) can be easily written as

$$\begin{aligned} B(f_x, f_y) \quad &= \quad \mathrm{E}\{\mathbf{a}_s^H(f_x, f_y)\, \mathbf{x}(n)\, \mathbf{x}(n)^H\, \mathbf{a}_s(f_x, f_y)\} \\ &= \quad \mathbf{a}_s^H(f_x, f_y)\, \mathbf{R}\, \mathbf{a}_s(f_x, f_y), \end{aligned} \tag{7}$$

where $\mathbf{R} = \mathrm{E}\{\mathbf{x}(n)\mathbf{x}(n)^H\}$ is the $MN \times MN$ covariance matrix of the transmitted waveforms. This yields a degree of freedom (DOF) of $\frac{(MN)^2+MN}{2}$. In the conventional transmit beampattern design problem, a covariance matrix, $\mathbf{R}$, is synthesized to match the transmitted power $B(\phi, \theta)$ to the desired beampattern which involves the minimization of the following cost function

$$\begin{aligned} J(\mathbf{R}) \quad = \quad & \sum_{l=1}^{L}\sum_{k=1}^{K} \Big| \mathbf{a}_s^H(f_x(l), f_y(k)) \mathbf{R} \mathbf{a}_s(f_x(l), f_y(k)) \\ & - \alpha P_d(f_x(l), f_y(k)) \Big|_2^2, \end{aligned} \tag{8}$$

where $P_d(f_x(l), f_y(k))$ is the desired beampattern defined over the two dimensional grid $\left(\{f_x(l)\}_{l=1}^{L}, \{f_y(k)\}_{k=1}^{K}\right)$ and α is a scaling factor. Since the matrix $\mathbf{R}$ is a covariance matrix, it should be positive semi-definite. Moreover, radio-frequency power amplifiers (RFPA) have limited dynamic range and they can not transmit all power levels with same power efficiency. If we want to design variety of transmit beampatterns without changing any hardware, RFPA should transmit same power levels for any beampattern. Therefore, to satisfy these constraints using the conventional methods, the minimization problem in (8) can be re-formulated as follows:

$$\begin{cases} \min\ J(\mathbf{R}) \\ \text{subject to} \\ \mathrm{C}_1:\ \mathbf{R} \succeq 0 \\ \mathrm{C}_2:\ R(n,n) = c,\ n = 1, 2, \ldots, MN. \end{cases} \tag{9}$$

C_1 represents the semi-definite constraint and C_2 ensures a uniform constant elemental power. The constrained problem in (9) can be optimally solved using an iterative SQP method. However, for large number of antennas the computational complexity of SQP method becomes prohibitively large. Therefore, such solutions are not feasible for planar-arrays of higher sizes. In order to reduce the computational cost by exploiting 2D-FFT algorithm, a closed-form solution to find the matrix $\mathbf{R}$ is proposed in the following section. The SQP algorithm is considered hereafter as a benchmark.

III. Proposed Covariance Matrix Design

For any $M \times N$ time domain matrix $\mathbf{H}_t$, $M \times N$ frequency domain matrix $\mathbf{H}_f$ can be easily generated. The relationship between the time domain coefficients $H_t(m, n)$ and the frequency domain coefficients $H_f(k_1, k_2)$ is given by the following 2D discrete-Fourier-transform (2D-DFT) formula

$$H_f(k_1, k_2) = \sum_{m=0}^{M-1}\sum_{n=0}^{N-1} H_t(m, n)\, e^{-j2\pi k_1 m/M} e^{-j2\pi k_2 n/N}. \tag{10}$$

Similarly, for given frequency domain coefficients, the time domain coefficients are obtained with the 2D inverse discrete-Fourier-transform (2D-IDFT) as follows

$$H_t(m, n) = \frac{1}{MN}\sum_{k_1=0}^{M-1}\sum_{k_2=0}^{N-1} H_f(k_1, k_2)\, e^{j2\pi k_1 m/M} e^{j2\pi k_2 n/N}. \tag{11}$$

Using (10) we obtain the following lemma

Lemma 1: Let $\mathbf{H}_f$ be an $M \times N$ matrix with real positive frequency domain coefficients and define the vectors $\mathbf{e}_M(k_1)$ and $\mathbf{e}_N(k_2)$ as

$$\begin{aligned} \mathbf{e}_M(k1) &= \begin{bmatrix} 1 & e^{j2\pi k_1/M} & \ldots & e^{j2\pi k_1(M-1)/M} \end{bmatrix}^T, \\ \mathbf{e}_N(k_2) &= \begin{bmatrix} 1 & e^{j2\pi k_2/N} & \ldots & e^{j2\pi k_2(N-1)/N} \end{bmatrix}^T, \end{aligned} \tag{12}$$

where $k_1 = 0, 1, \ldots, M-1$ and $k_2 = 0, 1, \ldots, N-1$. If we construct a matrix $\mathbf{R}_{hh}$ as

$$\mathbf{R}_{hh} = \frac{1}{(MN)^2}\sum_{k_1=0}^{M-1}\sum_{k_2=0}^{N-1} H_f(k_1, k_2)\, \mathbf{e}(k_1, k_2)\, \mathbf{e}^H(k_1, k_2), \tag{13}$$

where $\mathbf{e}(k_1, k_2) = \mathbf{e}_N(k_2) \otimes \mathbf{e}_M(k_1)$, then $\mathbf{R}_{hh}$ will be positive semi-definite and all of its diagonal elements will be equal. Moreover, the individual elements of $\mathbf{H}_f$ are related to the entries of $\mathbf{R}_{hh}$ using the following quadratic form

$$H_f(l_1, l_2) = \mathbf{e}^H(l_1, l_2) \mathbf{R}_{hh} \mathbf{e}(l_1, l_2). \tag{14}$$

The proof of *Lemma* 1 is given in the appendix.

Finding $\mathbf{R}_{hh}$ using (13) can be computationally very expensive since it requires the outer product of MN vectors and addition of MN matrices. To reduce the computational complexity, using (13), the individual elements of $\mathbf{R}_{hh}$ can be written as

$$\begin{aligned} R_{hh}(i_1, i_2) = \frac{1}{(MN)^2}\sum_{k_1=0}^{M-1}\sum_{k_2=0}^{N-1} & H_f(k_1, k_2) \\ & \times e^{j\frac{2\pi k_1 \langle i_1 - i_2 \rangle_M}{M}} e^{j\frac{2\pi k_2 (\lfloor i_1 \rfloor_M - \lfloor i_2 \rfloor_M)}{N}}, \end{aligned} \tag{15}$$

where $i_1, i_2 = 0, 1, \ldots, MN-1$. Comparing (15) with (11), we can write

$$R_{hh}(i_1, i_2) = \frac{1}{MN} H_t(\langle i_1 - i_2 \rangle_M, \lfloor i_1 \rfloor_M - \lfloor i_2 \rfloor_M). \tag{16}$$

As we know, for given frequency domain matrix $\mathbf{H}_f$, the time domain matrix $\mathbf{H}_t$ can be found using the FFT, therefore, finding $\mathbf{R}_{hh}$ using $\mathbf{H}_t$ is computationally less expensive. It should also be noted here that since $\mathbf{H}_f$ is real, $H_t(-m, -n) =$

$H_t^*(m,n)$, moreover, as $e^{-j\frac{2\pi k_1 m}{M}} = e^{j\frac{2\pi k_1 (M-m)}{M}}$ the matrix $\mathbf{R}_{hh}$ will be a block Toeplitz.

Note that the case of uniform linear array, studied in [15], can be considered as the special case of our proposed planar array with $N = 1$. In this case, the frequency and time domain matrices $\mathbf{H}_f$ and $\mathbf{H}_t$ are now reduced to $M \times 1$ vectors denoted respectively as $\mathbf{h}_f$ and $\mathbf{h}_t$. The correlation matrix $\mathbf{R}_{hh}$ becomes of dimensions $M \times M$ and by using formula (13) the individual elements of $\mathbf{R}_{hh}$ can be found as

$$\begin{aligned} R_{hh}(i_1,i_2) &= \frac{1}{M^2}\sum_{k_1=0}^{M-1} h_f(k_1) e^{\frac{2j\pi k_1 \langle i_1-i_2\rangle_M}{M}}, \\ &= \frac{1}{M^2}\sum_{k_1=0}^{M-1} h_f(k_1) e^{\frac{2j\pi k_1 (i_1-i_2)}{M}}. \end{aligned} \quad (17)$$

Similarly, using the fact that $\mathbf{h}_f$ is real, the matrix $\mathbf{R}_{hh}$ can be found using the time domain coefficients of $\mathbf{h}_f$ as

$$R_{hh}(i_1,i_2) = \frac{1}{M} h_t(i_1 - i_2). \quad (18)$$

Since $h_t(-i) = h_t^*(i)$, the matrix $\mathbf{R}_{hh}$ is the same Toeplitz matrix proposed in [15].

Since the matrix $\mathbf{R}_{hh}$ is positive semi-definite and all of its diagonal elements are equal, it satisfies both the C_1 and C_2 constraints of the optimization problem in (9) for designing the desired beampattern. Therefore, if $\mathbf{R}_{hh}$ is considered to be the waveform covariance matrix, by comparing (7) with (14), it can be easily noticed that the problem of transmit beampattern design can be mapped to the result obtained in the *Lemma* 1. This transformation only requires the mapping of steering vector $\mathbf{a}_s(f_x, f_y)$ to $\mathbf{e}(k1, k2)$. This can be done by mapping the values of f_x and f_y to k_1 and k_2 using the following expressions

$$\begin{cases} f_x \;\mapsto\; -0.5 + \frac{k_1}{M-1}, & k_1 = 0 \ldots M-1 \\ f_y \;\mapsto\; -0.5 + \frac{k_2}{N-1}, & k_2 = 0 \ldots N-1. \end{cases} \quad (19)$$

It should be noted here that using this mapping, f_x and f_y defining the desired beampattern, have discrete values. This can be a drawback for small antenna sized planar-arrays due to the small spatial resolution. In the proposed method, the desired beampattern will be defined in terms of f_x and f_y, however the beampattern in terms of spherical coordinates can be easily found using (4).

The two dimensional space can then be defined by a two dimensional grid $\left(\{(f_x)(l)\}_{l=1}^{M}, \{(f_y)(k)\}_{k=1}^{N}\right)$ represented by an $M \times N$ matrix $\mathbf{H}_f$. Thus, the entry $H_f(m,n)$ corresponds to $f_x = -0.5 + \frac{m}{M-1}$ and $f_y = -0.5 + \frac{n}{N-1}$. In order to define the ROI of the desired beampattern, we just have to assign 1 to the entries of $\mathbf{H}_f$ which are inside the ROI and 0 everywhere else. The different steps of our method are summarized in the following algorithm

TABLE I: Steps to compute $\mathbf{R}$

Step 0: Define $\mathbf{H}_f$ according to the ROI
Step 1: $\mathbf{H}_t \leftarrow$ 2D-IDFT($\mathbf{H}_f$)
Step 2: Compute $\mathbf{R}_{hh}$ using (16)
Step 3: Use $\mathbf{R}_{hh}$ as the waveform covariance matrix $\mathbf{R}$

It is worth noting that different forms of beampatterns can be obtained by changing the coefficients of the matrix $\mathbf{H}_f$ as shown in Fig. 2. For example, a circular shaped beam can be designed by filling $\mathbf{H}_f$ with ones and zeros as shown in the figure and finally following the steps of TABLE I to obtain the corresponding waveform covariance matrix.

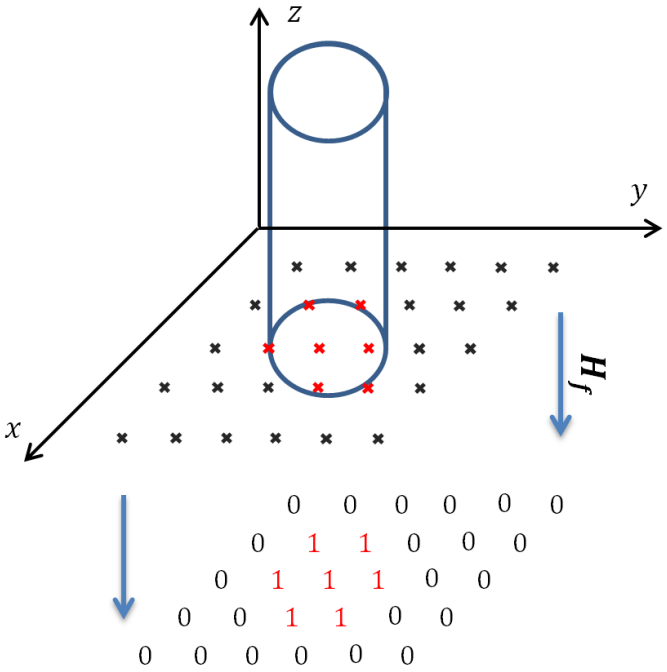

Fig. 2: Circular shaped beampattern.

IV. Computational Complexity

As we can notice from TABLE I, the only computational complexity of the proposed method comes from the IDFT computation step. The NM IDFT coefficients are computed using one of the famous FFT algorithms which have a complexity equal to $O(MN\ \log(MN))$ computations. However, the SQP method used in Sec. II has a complexity of the order $O(\log(\frac{1}{\eta})\ (MN)^{3.5})$ for a given accuracy η [17]. As shown in Fig. 3, the gap of computational complexity between the FFT-based and SQP-based algorithms increases with the number of antennas which makes our method more suitable for real time radar applications.

Once the covariance matrix is designed, in the next step, waveforms to realise this covariance matrix are designed. To design waveforms most of the proposed algorithms are iterative and their computational complexity is high. In the following, the proposed novel algorithm does not require the design of waveforms covariance matrix rather it can directly design the waveforms in closed form for the given desired beampattern. This further reduces the computational complexity of the beampattern design.

V. Direct Design of Waveforms for the Desired Beampattern

In this section, a closed-form expression to directly design the waveforms for the desired beampattern is proposed. We

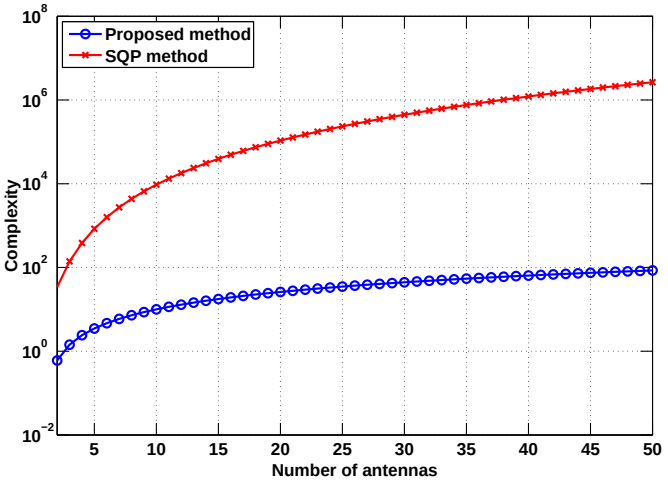

Fig. 3: Computational complexity comparison between the FFT-based algorithm and the SQP method.

start from (13), which can also be written as

$$R(i_1,i_2) = \sum_{k_1=0}^{M-1}\sum_{k_2=0}^{N-1}\left(\frac{\sqrt{H_f(k_1,k_2)}}{MN}e^{j\frac{2\pi k_1\langle i_1\rangle_M}{M}}e^{j\frac{2\pi k_2\lfloor i_1\rfloor_M}{N}}\right) \times \left(\frac{\sqrt{H_f(k_1,k_2)}}{MN}e^{j\frac{2\pi k_1\langle i_2\rangle_M}{M}}e^{j\frac{2\pi k_2\lfloor i_2\rfloor_M}{N}}\right)^*. \quad (20)$$

Assuming $k = k_1 + Mk_2 = \langle k\rangle_M + M\lfloor k\rfloor_M$, both terms in the above equation can be considered as the kth elements of the waveforms $\mathbf{s}_{i_1}$ and $\mathbf{s}_{i_2}$ that can be written as

$$\begin{aligned} s_{i_1}(k) &= \frac{\sqrt{H_f(\langle k\rangle_M,\lfloor k\rfloor_M)}}{MN}e^{j\frac{2\pi\langle k\rangle_M\langle i_1\rangle_M}{M}}e^{j\frac{2\pi\lfloor k\rfloor_M\lfloor i_1\rfloor_M}{N}}, \\ s_{i_2}(k) &= \frac{\sqrt{H_f(\langle k\rangle_M,\lfloor k\rfloor_M)}}{MN}e^{j\frac{2\pi\langle k\rangle_M\langle i_2\rangle_M}{M}}e^{j\frac{2\pi\lfloor k\rfloor_M\lfloor i_2\rfloor_M}{N}}, \end{aligned}$$

where $k = 0,1,\ldots,MN-1$. Thus, the cross-correlation between the waveforms $\{s_{i_1}(k)\}$ and $\{s_{i_2}(k)\}$ can be written as

$$R(i_1,i_2) = \sum_{k=0}^{MN-1} s_{i_1}(k)\, s_{i_2}(k)^*. \quad (21)$$

The corresponding waveform vector can be written as

$$\mathbf{s}_i = \begin{bmatrix} \frac{\sqrt{H_f(0,0)}}{MN}e^{j\frac{2\pi(0)\lfloor i\rfloor_M}{N}}e^{j\frac{2\pi(0)\langle i\rangle_M}{M}} \\ \vdots \\ \frac{\sqrt{H_f(0,N-1)}}{MN}e^{j\frac{2\pi(N-1)\lfloor i\rfloor_M}{N}}e^{j\frac{2\pi(0)\langle i\rangle_M}{M}} \\ \vdots \\ \vdots \\ \frac{\sqrt{H_f(M-1,0)}}{MN}e^{j\frac{2\pi(0)\lfloor i\rfloor_M}{N}}e^{j\frac{2\pi(M-1)\langle i\rangle_M}{M}} \\ \vdots \\ \frac{\sqrt{H_f(M-1,N-1)}}{MN}e^{j\frac{2\pi(N-1)\lfloor i\rfloor_M}{N}}e^{j\frac{2\pi(M-1)\langle i\rangle_M}{M}} \end{bmatrix} = \begin{bmatrix} \mathbf{v}_0^i \\ \vdots \\ \mathbf{v}_{M-1}^i \end{bmatrix} \quad (22)$$

where

$$\mathbf{v}_p^i = \begin{bmatrix} \frac{1}{MN}\sqrt{H_f(p,0)}e^{j\frac{2\pi(0)\lfloor i\rfloor_M}{N}}e^{j\frac{2\pi p\langle i\rangle_M}{M}} \\ \vdots \\ \frac{1}{MN}\sqrt{H_f(p,N-1)}e^{j\frac{2\pi(N-1)\lfloor i\rfloor_M}{N}}e^{j\frac{2\pi p\langle i\rangle_M}{M}} \end{bmatrix}, \quad (23)$$

while $p = 0,1,\ldots,M-1$. Therefore, for any transmitting element of the rectangular array at location (m,n) where $m = 0\ldots M-1$ and $n = 0\ldots N-1$, we assign the waveform $\mathbf{s}_i$ defined in (22) with $i = m + nM$. It should be noted here that depending on the desired beampattern some elements of the waveform $\mathbf{s}_i$ may be equal to zero.

A. Peak to Average Power Ratio

We investigate hereafter the performance of our waveform design method in terms of PAPR. If N_a is the number of non-zero elements in the matrix $\mathbf{H}_f$, the ith waveform will be transmitting N_a non-zero symbols. Therefore, the average transmitted power from the (m,n)th antenna can be written as

$$\begin{aligned} P_i(\text{avg}) &= \frac{1}{N_a}\mathbf{s}_i^H\mathbf{s}_i, \\ &= \frac{1}{N_a}\sum_{k=0}^{MN-1}\frac{1}{(MN)^2}s_i(k)s_i^*(k), \\ &= \frac{N_a}{N_a(MN)^2}. \end{aligned}$$

We note that the average transmitted power does not depend on the antenna location, which confirms that the uniform elemental power constraint is satisfied. Similarly, the peak power of the ith waveform can be derived as

$$\begin{aligned} P_i(\text{peak}) &= \max_k\left|\frac{\sqrt{H_f(\langle k\rangle_M,\lfloor k\rfloor_M)}}{MN}e^{j\frac{2\pi\langle k\rangle_M\langle i\rangle_M}{M}} e^{j\frac{2\pi\lfloor k\rfloor_M\lfloor i\rfloor_M}{N}}\right|^2, \\ &= \max_k\left|\frac{H_f(\langle k\rangle_M,\lfloor k\rfloor_M)}{(MN)^2}\right| = \frac{1}{(MN)^2}. \quad (24) \end{aligned}$$

Therefore, the PAPR can be found as

$$\text{PAPR} = \frac{P_i(\text{peak})}{P_i(\text{avg})} = \frac{1/(MN)^2}{1/(MN)^2} = 1. \qquad (25)$$

From (25), it can be noted that PAPR is equal to one for any antenna.

VI. NUMERICAL SIMULATIONS

In this section, the performance of the proposed FFT-based algorithm is investigated. For simulation, a rectangular planar array composed of $M \times N$ antennas is considered. The spacing between any two adjacent antennas on the $x-$ and $y-$axis of the planar-array is kept $\lambda/2$. The MSE between the desired and designed beampatterns is defined as

$$\text{MSE} = \sum_{l=1}^{L}\sum_{k=1}^{K} |\mathbf{a}_s^H(f_x(l), f_y(k))\mathbf{R}\mathbf{a}_s(f_x(l), f_y(k)) - \alpha P_d(f_x(l), f_y(k))|^2/KL.$$

In the first simulation, the ROI is defined as $-0.1 \leq f_x \leq 0.1$ and $-0.1 \leq f_y \leq 0.1$ and we use $N = M = 10$. To design this beampattern, first we synthesise $\mathbf{R}$ using SQP method proposed in [8]. The designed beampattern using the synthesised covariance matrix is shown in Fig. 4, which is the best possible designed beampattern. Note that the beampattern is normalized by dividing by α. For this simulation, the total number of antennas is 100, therefore, to synthesise covariance matrix, the simulation is very time consuming. Here, the actual waveforms to realise the synthesised covariance matrix are not designed as they also require very high computational complexity iterative algorithm. The designed beampattern with the actual waveforms may be degraded too. In order to reduce the computational complexity to design the desired beampattern, we use in the second simulation our proposed closed-form 2D-FFT based low complexity algorithm with the same number of antennas $N = M = 10$. The corresponding designed beampattern, using the covariance matrix $\mathbf{R}$ obtained by our proposed algorithm, is shown in Fig. 5. The designed beampattern shown is the beampattern of covariance matrix. To design this beampattern, the algorithm to directly design the waveforms is proposed in Sec. V.

In order to compare the performance of the two algorithms shown in the previous two simulations, we compare the corresponding MSE for different planar array dimensions and for an ROI defined by $-0.1 \leq f_x \leq 0.1$ and $-0.1 \leq f_y \leq 0.1$. As shown in Fig. 6, the MSE of both methods is plotted in function of the total number of antennas MN corresponding to a rectangular array of dimension $M \times N$. We note that for low number of antennas the performance of the FFT-based method is affected. This is due to the fact that the ROI (represented by the matrix $\mathbf{H}_f$) is constructed in the two dimensional grid $\left(\{(f_{k1})_l\}_{l=1}^{M}, \{(f_{k2})\}_{k=1}^{N}\right)$ whose resolution is related to the number of antennas. However, as the dimensions of the rectangular array increase the proposed method achieves lower MSE level approaching the SQP-based method with the advantage of being much less complex as illustrated in Fig. 3.

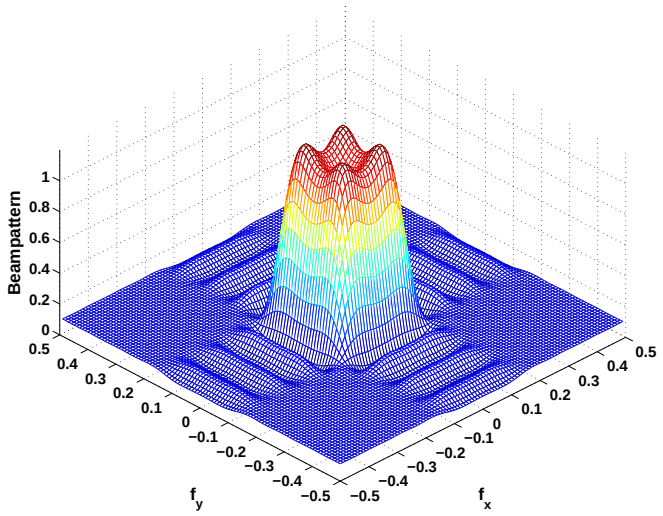

Fig. 4: The designed beampattern using SQP based method. Here the ROI is $-0.1 \leq f_x \leq 0.1$ and $-0.1 \leq f_y \leq 0.1$ and $M = N = 10$.

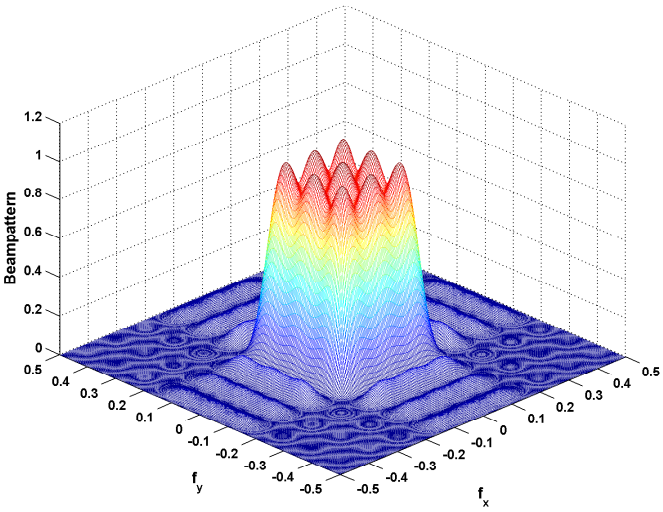

Fig. 5: The designed beampattern using the proposed FFT-based algorithm. Here, the ROI is $-0.1 \leq f_x \leq 0.1$ and $-0.1 \leq f_y \leq 0.1$ and $M = N = 10$.

Next, we perform various beampattern shape design by manipulating the ROI and plugging it into the FFT-based algorithm described in TABLE I to obtain the corresponding covariance matrix. The shape of the beampattern is determined by the ROI, which is defined by the positions of the non zero coefficients in the matrix $\mathbf{H}_f$. Note that in order to obtain good results the symmetry of the beampattern must be respected. Figs. 7-10 show some of the various beampattern configurations that can be designed using a planar array of dimensions $N = M = 20$. For display purposes, we only show a two dimensional graph representing the projection of

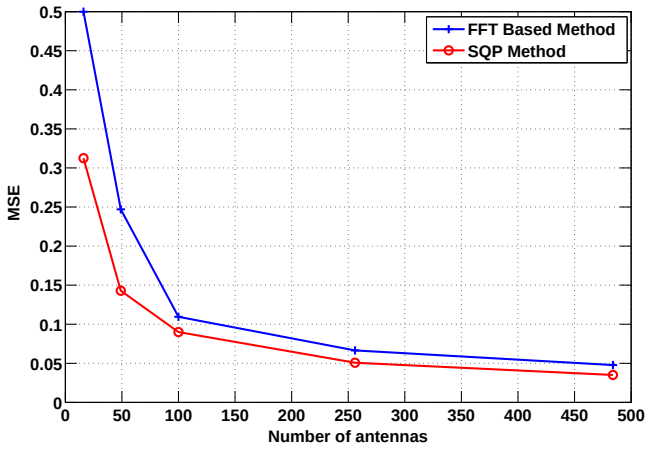

Fig. 6: MSE comparison between the FFT-based algorithm and the SQP method for different planar array dimensions.

the designed beampattern in the $(f_x - f_y)$ plane. In Fig. 7 the transmitted power is focused only in the corners. Fig. 8 shows the beampattern obtained when we want to transmit only on the borders. Fig. 9 shows a beampattern which is focused both in the borders and in the center. Finally, Fig. 10 shows a circular shaped beampattern as illustrated in Fig. 2.

In the final simulation, a linear array of 10 antenna is used. To transmit the power between the azimuth angle -30° and 30°, waveforms are directly designed using our proposed algorithm and the algorithm in [12]. The simulation results are shown in Fig. 11. It can be seen in the figure that the algorithm in [12] yields almost uniform transmit power in the ROI, however, the designed beampattern has slower roll-off and higher side-lobe-levels compared to our proposed algorithm. An other advantage of using our proposed algorithm is that it generates finite alphabet symbols for each waveform.

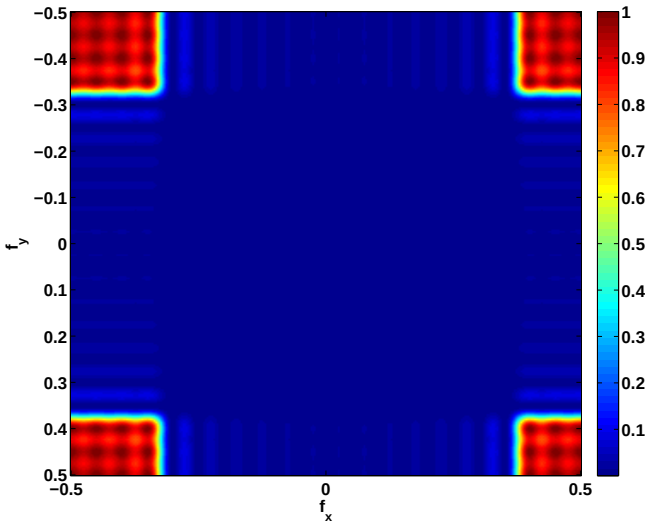

Fig. 7: FFT-based transmit Beampattern, $N = M = 20$, ROI focused in the corners.

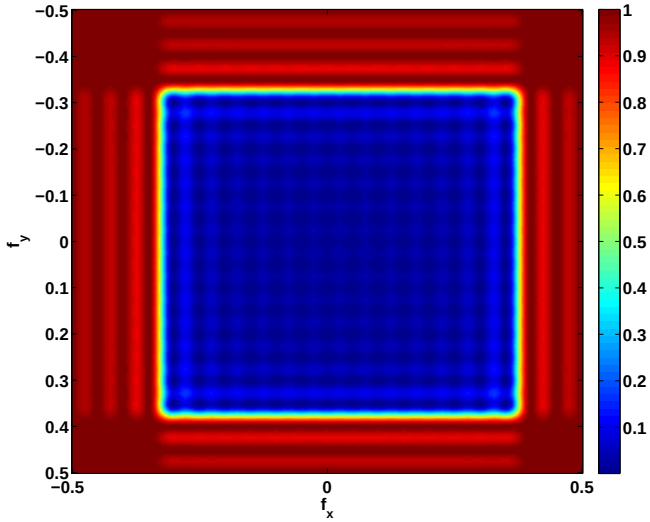

Fig. 8: FFT-based transmit Beampattern, $N = M = 20$, ROI focused in the borders.

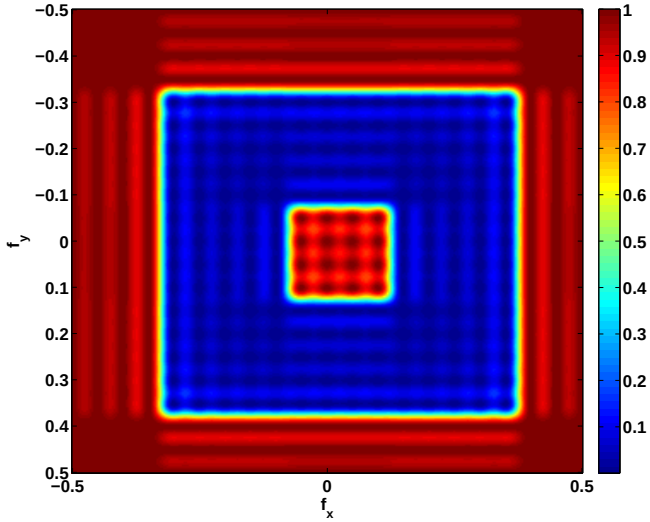

Fig. 9: FFT-based transmit beampattern design, $N = M = 20$. Here, the transmitted power needs to be focused in the center and the borders.

VII. Conclusion

In this paper we have presented a closed-form method of covariance matrix design for the planar MIMO transmit beamforming problem that exploits the IDFT coefficients. The positive semi-definition and uniform element power constraints are verified by the designed matrix. Next, a method of direct waveform design exploiting the expression of the covariance matrix that we found is proposed. The numerical simulations presented confirm that the proposed method is computationally efficient and performs closely to the SQP-based method as the number of antennas increases. As a future work, we will study an On-Off scheme which will use the minimum number of antennas for a given beampattern.

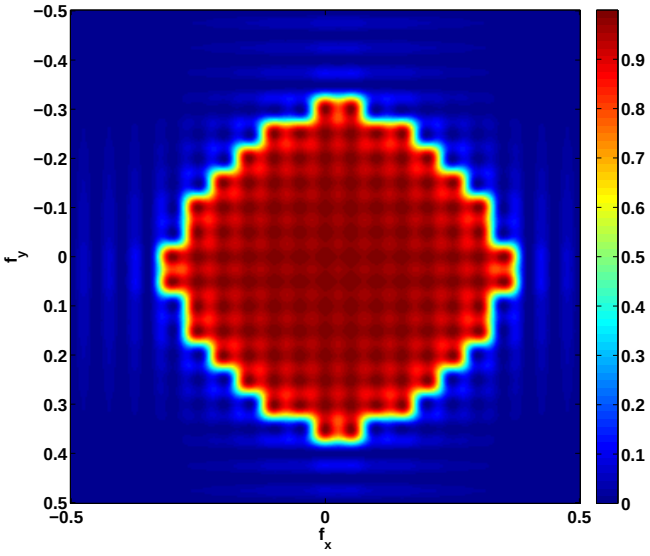

Fig. 10: FFT-based transmit beampattern design, $N = M = 20$. Here, the ROI has a circular shape.

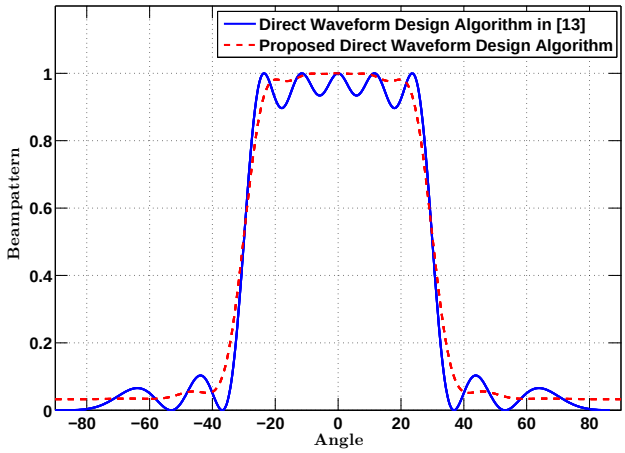

Fig. 11: Comparison of direct waveform design methods for the desired beampattern using linear array. Here, in both algorithms each waveform transmits 10 symbols.

APPENDIX

The proof of *Lemma* 1 is straightforward. By exploiting the orthogonality of the vectors defined in (12), we have $\mathbf{e}^H(l_1,l_2)\mathbf{e}(m_1,m_2) = (MN)^2\delta_{l_1m_1}\delta_{l_2m_2}$ where δ_{ij} in the Kronecker delta. Thus, we obtain

$$\begin{aligned}\mathbf{e}^H(l_1,l_2)\mathbf{R}_{hh}\mathbf{e}(l_1,l_2) &= \frac{1}{(MN)^2}\sum_{k_1=0}^{M-1}\sum_{k_2=0}^{N-1}\mathbf{H}_f(k_1,k_2)\\ &\quad \mathbf{e}^H(l_1,l_2)\mathbf{e}(k_1,k_2)\mathbf{e}^H(k_1,k_2)\mathbf{e}(l_1,l_2)\\ &= \frac{1}{(MN)^2}\sum_{k_1=0}^{M-1}\sum_{k_2=0}^{N-1}\mathbf{H}_f(k_1,k_2)\\ &\quad (MN)^2\delta_{l_1k_1}\delta_{l_2k_2}\\ &= \mathbf{H}_f(l_1,l_2).\end{aligned}$$

Since $\mathbf{H}_f(k_1,k_2) \geq 0$ for $k_1 = 0,1,\ldots,M-1$ and $k_2 = 0,1,\ldots,N-1$ and $\mathbf{R}_{hh}$ is the sum of multiple rank 1 positive semi-definite matrices, $\mathbf{R}_{hh}$ is positive semi-definite.

To prove that all the diagonal elements of $\mathbf{R}_{hh}$ are equal, let us find the expression the ith diagonal element $\mathbf{R}_{hh}(i,i)$ from the formula in (13)

$$\begin{aligned}\mathbf{R}_{hh}(i,i) &= \frac{1}{(MN)^2}\sum_{k_1=0}^{M-1}\sum_{k_2=0}^{N-1}\mathbf{H}_f(k_1,k_2)\\ &\quad \left[\mathbf{e}(k_1,k_2)\,\mathbf{e}^H(k_1,k_2)\right](i,i).\end{aligned}$$

Since $\left[\mathbf{e}(k_1,k_2)\,\mathbf{e}^H(k_1,k_2)\right](i,i) = 1$ for any index value i, we can write

$$\begin{aligned}\mathbf{R}_{hh}(i,i) &= \frac{1}{(MN)^2}\sum_{k_1=0}^{M-1}\sum_{k_2=0}^{N-1}\mathbf{H}_f(k_1,k_2)\\ &= \frac{N_a}{(MN)^2},\end{aligned} \tag{26}$$

where N_a is the number non-zero elements in the frequency domain matrix $\mathbf{H}_f$.

REFERENCES

[1] E. Fishler, A. Haimovich, R. Blum, D. Chizhik, L. Cimini, and R. Valenzuela, "MIMO radar: An idea whose time has come," in *Proceedings of the IEEE Radar Conference,*, pp. 71–78, April 2004.

[2] L. Xu, J. Li, and P. Stoica, "Target detection and parameter estimation for MIMO radar systems," *IEEE Transactions on Aerospace and Electronic Systems,*, vol. 44, pp. 927–939, July 2008.

[3] A. Hassanien and S. Vorobyov, "Phased-MIMO radar: A tradeoff between phased-array and MIMO radars," *IEEE Transactions on Signal Processing,*, vol. 58, pp. 3137–3151, June 2010.

[4] A. Haimovich, R. Blum, and L. Cimini, "MIMO radar with widely separated antennas," *IEEE Signal Processing Magazine,*, vol. 25, no. 1, pp. 116–129, 2008.

[5] J. Li and P. Stoica, "MIMO radar with colocated antennas," *IEEE Signal Processing Magazine,*, vol. 24, pp. 106–114, Sept 2007.

[6] E. Fishler, A. Haimovich, R. Blum, L. Cimini, D. Chizhik, and R. Valenzuela, "Spatial diversity in radars-models and detection performance," *IEEE Transactions on Signal Processing,*, vol. 54, pp. 823–838, March 2006.

[7] D. Fuhrmann and G. San Antonio, "Transmit beamforming for MIMO radar systems using signal cross-correlation," *IEEE Transactions on Aerospace and Electronic Systems,*, vol. 44, pp. 171–186, January 2008.

[8] P. Stoica, J. Li, and Y. Xie, "On probing signal design for MIMO radar," *IEEE Transactions on Signal Processing,*, vol. 55, pp. 4151–4161, Aug 2007.

[9] T. Aittomaki and V. Koivunen, "Signal covariance matrix optimization for transmit beamforming in MIMO radars," in *Conference Record of the Forty-First Asilomar Conference on Signals, Systems and Computers,*, pp. 182–186, Nov 2007.

[10] T. Aittomaki and V. Koivunen, "Low-complexity method for transmit beamforming in MIMO radars," in *IEEE International Conference on Acoustics, Speech and Signal Processing,*, vol. 2, pp. II–305–II–308, April 2007.

[11] S. Ahmed, J. Thompson, Y. Petillot, and B. Mulgrew, "Unconstrained synthesis of covariance matrix for MIMO radar transmit beampattern," *IEEE Transactions on Signal Processing,*, vol. 59, pp. 3837–3849, Aug 2011.

[12] D. Fuhrmann, J. Browning, and M. Rangaswamy, "Signaling strategies for the hybrid MIMO phased-array radar," *IEEE Journal of Selected Topics in Signal Processing,*, vol. 4, pp. 66–78, Feb 2010.

[13] W.-Q. Wang, "MIMO SAR Chirp modulation diversity waveform design," *IEEE Geoscience and Remote Sensing Letters,*, vol. 11, pp. 1644–1648, Sept 2014.

[14] D. Fuhrmann and G. San Antonio, "Transmit beamforming for MIMO radar systems using partial signal correlation," in *Conference Record of the Thirty-Eighth Asilomar Conference on Signals, Systems and Computers,*, vol. 1, pp. 295–299 Vol.1, Nov 2004.

[15] J. Lipor, S. Ahmed, and M.-S. Alouini, "Fourier-based transmit beampattern design using MIMO radar," *IEEE Transactions on Signal Processing,*, vol. 62, pp. 2226–2235, May 2014.

[16] P. Stoica, J. Li, X. Zhu, and B. Guo, "Waveform synthesis for diversity-based transmit beampattern design," in *IEEE/SP 14th Workshop on Statistical Signal Processing,*, pp. 473–477, Aug 2007.

[17] S. Ahmed, J. Thompson, Y. Petillot, and B. Mulgrew, "Finite alphabet constant-envelope waveform design for MIMO radar," *IEEE Transactions on Signal Processing,*, vol. 59, pp. 5326–5337, Nov 2011.

[18] D. Fuhrmann, J. Browning, and M. Rangaswamy, "Constant-modulus partially correlated signal design for uniform linear and rectangular MIMO radar arrays," in *International Waveform Diversity and Design Conference,*, pp. 197–201, Feb 2009.